FFEMS Fatigue & Fracture of Engineering Materials & Structures
ORIGINAL CONTRIBUTION
doi: 10.1111/ffe.12275

Micronotches for studying growth of small cracks

W. WESSEL[1], J. MILDNER[2], P. PITZ[1], A. BRUECKNER-FOIT[1], M. WOLLENHAUPT[2,3] and T. BAUMERT[2]

[1]*Institute for Materials Engineering, University of Kassel, Kassel, Germany*, [2]*Department of Physics and CINSaT, University of Kassel, Kassel, Germany*, [3]*Department of Physics, Carl von Ossietzky University of Oldenburg, Oldenburg, Germany*

Received Date: 4 September 2014; Accepted Date: 6 November 2014; Published Online: 19 December 2014

ABSTRACT Well-defined starter cracks at preselected sites in the microstructures are needed for systematic investigation of the characteristic features of microstructure controlled growth of small cracks. A kinked ellipsoidal micronotch with very high notch factor at the trailing kink is proposed, which triggers controlled crack initiation along the notch contour. These micronotches can be machined by femtosecond laser ablation with virtually no heat-affected zone at the edges. Crack growth results obtained for an intermetallic γ-TiAl alloy are presented as an illustrative example.

Keywords crack initiation and propagation; fatigue crack growth; intermetallic compound; microcrack; notched specimen.

NOMENCLATURE

a = crack (notch) depth
b = notch width
c = half length of surface crack (notch)
da/dN = crack growth rate
ΔK = range of stress intensity factor
ε = strain
σ = stress

INTRODUCTION

Fracture mechanics methods for generating valid crack growth data for long cracks are well-established and are widely used both in research and in industrial application. However, a large part of the lifetime of a component subjected to fatigue loading is spent in the small crack regime in which cracks strongly interact with the microstructure and long-crack data are not applicable.

It is common practice to gather information about the small crack regime using smooth specimen with cracks being initiated at natural defects. This has the advantage that the shape of the cracks is similar to those found under service conditions in the actual component. On the other hand, initial conditions and boundary conditions are not always well-defined, which, in turn, may lead to difficulties when analysing the crack growth data. Additionally, other factors can impede observation of stable crack growth. A typical scenario is the following: When a material system is under development, it may still contain comparatively large defects (e.g. pores from insufficient densification), which cause failure after comparatively few load cycles. Even though it is obvious that these defects will be eventually removed by optimizing the processing routine, it is not possible at this stage to estimate the material's potential resistance against stable extension of small cracks, unless a starter crack is introduced from which small cracks are initiated more rapidly than from the fabrication defects in question.[1] Graded materials or material joints represent another case in which local crack growth data are needed. Initiation and growth of small cracks can normally readily be observed in one phase (the soft one in general), but no observable cracks can be initiated in any of the other phases prior to failure of the specimen.[2] Yet, another example is crack growth starting from internal cracks. Recently, this phenomenon has gained increased attention within the framework of understanding very high cycle fatigue[3] as the crack growth rates of internal cracks can be determined experimentally by doing experiments in vacuum with artificial surface cracks of the same size as the natural cracks.

Small artificial crack-initiating notches are required to solve these problems. The size of these 'crack starters' has to be comparable to the length scale of the microstructure, and it should be possible to place them in the vicinity to

Correspondence: A. Brueckner-Foit. E-mail: a.brueckner-foit@uni-kassel.de

microstructural features of interest. A classical paper on this subject is that in Ref. [4] where attempts were made to start small cracks from surface pits introduced by electrodischarging or by laser machining. These attempts failed because of secondary cracks (electrodischarging) or because of thermal interaction with the adjacent material (laser machining). In case of laser machining, a nanosecond laser with pulse duration of 3 ns was used, leading to round 'pits' with a diameter of 20–40 µm and a heat-affected zone of a few micrometres. In a more recent approach, controlled initiation of microcracks was achieved by introducing micronotches using focused ion beam (FIB) machining.[5,6] These notches were placed at preselected microstructural features such as grain boundaries, and controlled microstructurally dominated crack growth was observed. However, this method is rather time-consuming. Moreover, the size of the specimen is limited because of the restriction imposed by the FIB equipment. An alternative approach is micromachining using femtosecond (fs) laser ablation.[1,7–10] An experimental technique for defining micronotches from which short edge cracks could be initiated is described in Ref. [11]. At first, an edge cut is introduced using a razor blade, and an FIB cut is placed at the notch tip in order to obtain a sufficiently sharp notch tip. Compression precracking, which is widely used for studying crack growth in the threshold region of long cracks (see, e.g. Ref. [12]), could also be used if the edge cut is large enough.

In all these cases, the notch geometries used were fairly simple as the materials in question were quite ductile, and a comparatively moderate stress concentration at the notch tip was sufficient to trigger localized slip and eventually crack initiation. More sophisticated notch geometries are called for, if the material in question is highly notch sensitive with low fracture toughness and has high crack growth rates. This problem is addressed in this paper. In the first section, notch manufacturing by fs laser ablation is briefly described, and the geometry of the starter notch is defined. Then, the experimental methods used in the fatigue tests are explained. The section on MICROCRACK INITIATION AND GROWTH contains some crack growth data obtained with these methods.

DEFINITION OF MICRONOTCHES

Femtosecond laser beams with ultrashort laser pulses of high energy density can be used for material machining with extremely high precision.[13–15] Virtually, no heat-affected zone is formed at the edge of the ablation zone because of the extremely short duration of the pulse. This is related to the fact that there is reduced energy diffusion in the lattice during machining in contrast to machining with conventional nanosecond and picosecond lasers. During such an ultrashort pulse, the material is directly ablated as plasma, which moves away from the ablation spot in a unidirectional manner. If the remaining debris is removed, for example, by a constant air flow, very steep edges can be made with negligible heat-affected zones.

Hence, notches of predefined shapes can be placed in a material using fs laser machining. Figure 1 gives an overview of the experimental set-up, which is described as follows: The fs laser system consists of a Ti : Sapphire femtosecond oscillator (Femtosource Scientific Pro, Femtolasers, Vienna, Austria) and a Chirped-Pulse Multipass Amplifier (Femtopower Pro, Femtolasers). Pulses of 800 mW with duration of 35 fs and a wavelength of 790 nm are generated at a repetition rate of 1 kHz. Single-shot control of the laser system enables different operation modes, that is, single-shot, multishot and kHz mode. The laser radiation is guided to a modified microscope using a mirror system. A coupling mirror within the tube of the microscope allows changing between observation mode (for specimen positioning and observation) and fs pulse mode. The positioning accuracy of the system is 10 nm. The incoming fs pulses are then

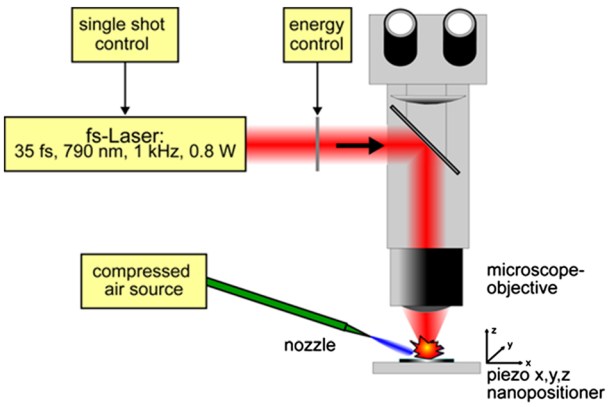

Fig. 1 Schematic set-up of the fs-laser-machining device.

focused through a microscope objective (50×, N.A. 0.5) onto the sample. As the energy of the laser pulse exceeds the threshold for material ablation, the material is directly transferred into a plasma state.

For a given sample system, the amount of ablated material depends on the energy and the pulse duration applied. One shot produces a semispherical hole of about 1.4–1.6 μm diameter with the parameters described in Ref. [1] for the intermetallic TiAl alloy considered in this study. A larger volume of material is removed by placing shots next to each other and by repeated ablation at the same point. Moving the sample relative to the laser focus according to a predefined trajectory, different notch shapes can be manufactured. To remove the ablated material properly, a continuous airflow is applied to the interaction region via a combined set-up of a micronozzle and compressed air. This machining method has the advantage of being very versatile with respect to notch shapes both on the surface and in depth direction as well as fast processing times. Operating in kHz mode, the machining time for one kinked elliptical notch (see details later in the text) is about 6:40 min, for one V-shaped notch about 8 min. One can achieve even shorter processing times with higher repetition rates and a more sophisticated triggering.

Two geometries of micronotches are considered in this study. The first one is a V-shaped notch with a hexagonal extension on the surface (Fig. 2). This notch was machined by ablating similar hexagons with decreasing area in depth direction. This notch shape was defined because of its angular shape, which leads to comparatively high notch factors in any potential extension direction and hence is suitable for surface or in-depth initiation of a crack.

The second notch was defined using the line of thinking that was originally used for the chevron notch in ceramic materials.[16] A trailing kink in the notch line leads to very high notch factors. Consequently, a crack is very likely to be initiated at this point. The first regime of stable crack extension will be spent in smoothing the notch front, and a sharp well-defined crack front will develop in the specimen. This idea, which had originally been developed for generating through-wall cracks in ceramic materials, was transferred to the case of the surface cracks. Hence, a micronotch was defined with a trailing kink along the notch front with a shape as shown in Fig. 3.

This kinked ellipsoidal micronotch was machined by ablating first narrowing elliptical contours with relatively high ablation energy (1.2 μJ) in the deep section of the notch and then wider ellipses with reduced ablating energy (200 nJ) in the shallow section of the notch with the goal of increasing the machining accuracy and of sharpening the edges.

A finite element analysis using ABAQUS code (Fig. 4) was employed for determining the stress concentration factors along the notch contour with the rounding of the sharp notch tips caused by the minimum ablation volume taken into account. Adaptive meshing was used with the refinement of the tetragonal elements limited both at the notch contour and at the boundary. The notch geometry was selected as $2c = 130\,\mu m$, $a = 55\,\mu m$ and $b = 35\,\mu m$ for both notches. The V-shaped part of the notch in Fig. 2 had a length of 20 μm, whereas the kink of the notch geometry shown in Fig. 3 was located at a distance

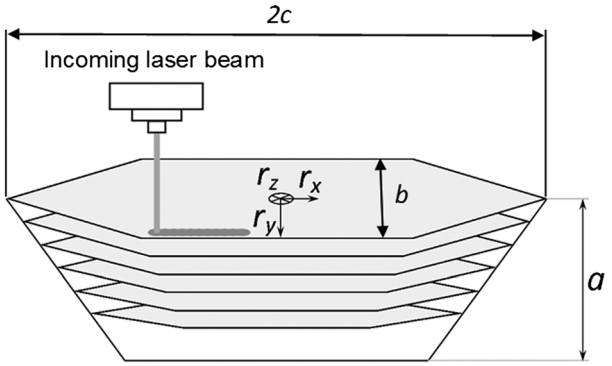

Fig. 2 V-shaped notch with schematic machining sequence (top view and side view with schematic illustration of successive layers).

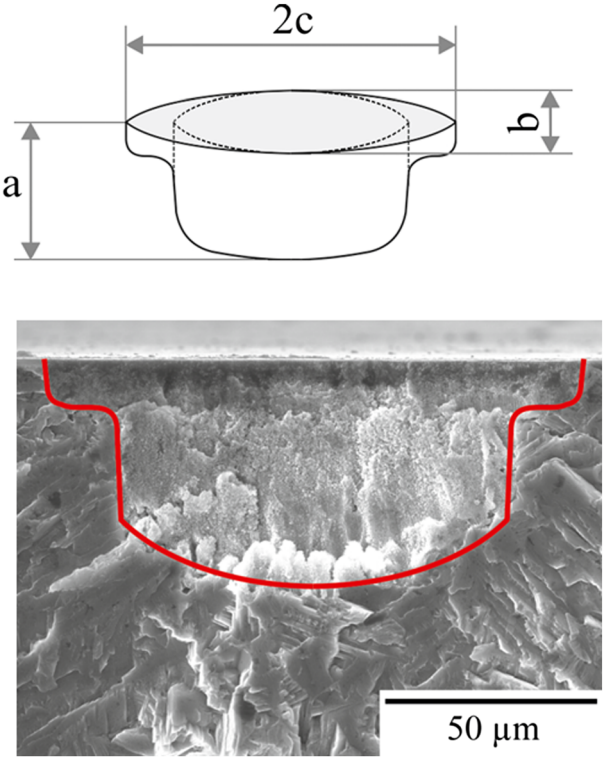

Fig. 3 Kinked elliptical notch. (a) Design geometry (top view and side view). (b) Realization using fs laser machining.

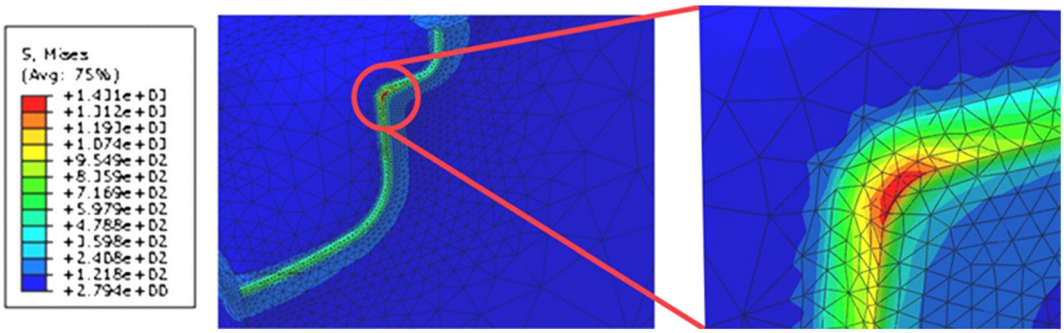

Fig. 4 Stress field in the vicinity of the trailing edge of the kinked elliptical notch (100 MPa nominal load).

of 12 μm from the surface and 20 μm from the notch tip. Linear elastic isotropic material behaviour was used in both cases, and the *c*-axis of the notch was placed perpendicular to the loading direction.

The stress concentration factor (defined as local von Mises stress value divided by nominal stress value) along the notch contour had maximum values of around 6.2 at the notch tips for the V-notch, whereas values as high as 14.3 were obtained at the trailing edge of the kinked elliptical notch (Fig. 4). Typical notch geometries had lengths between 80 and 140 μm with the depth varying from 10 to 40 μm. The width varied with the depth because of manufacturing restrictions; an opening ratio of $a/b = 1$ or less was achieved in all cases. These dimensions are the ones that lead to successful starter cracks in the case of the fully lamellar γ-TiAl studied in the succeeding

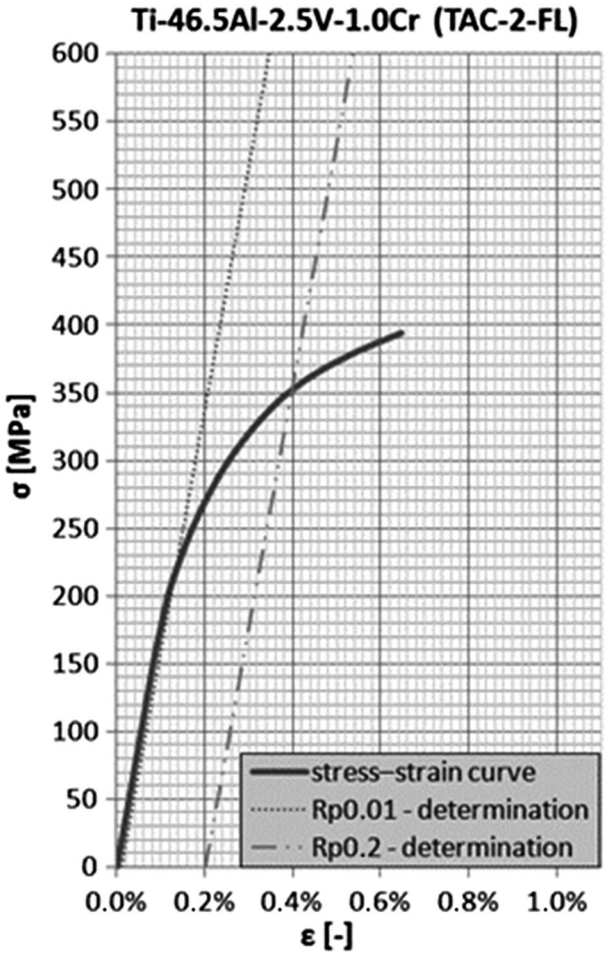

Fig. 5 Stress–strain curve: Ti-46.5Al-2.5V-1.0Cr in fully lamellar condition.

text. Smaller notches can be manufactured with the limitation being the single-shot ablation volume of the minimum pulse energy necessary for ablation, but no cracks will be initiated in this case as it was shown in Ref. [17]. A finite notch width of 10 to 40 µm has to be chosen for machining purposes.

The maximum stress concentration factor of the kinked ellipsoidal notch is located at the trailing kink as it was anticipated. Crack initiation is very likely to start here. The crack front will progress in a controlled manner until a smooth notch/crack contour of approximately semi-elliptical shape is reached. It is then very easy to initiate a semi-elliptical surface crack, as there is already a sharp crack tip at some part of the notch contour. Different locations of the kink along the notch contour can be machined easily by changing the computer-controlled ablation path and/or the ablation energy conferred on the material by the laser.

FATIGUE TESTS

The usefulness of the optimized micronotch in studying extension of small cracks is illustrated using an intermetallic γ-TiAl alloy in fully lamellar condition. The size of the lamellae colonies varied between 100 and 1500 µm (in the direction of the lamellae orientation). This material has very limited ductility at room temperature as it can be seen from the stress–strain curve given in Fig. 5 and a fracture toughness of about 10 MPa$\sqrt{\text{m}}$.

Consequently, this material is very notch-sensitive. Additional difficulties for observing stable crack extension stem from the fact that this material system is still under development and frequently contains pores or other natural defects causing failure. At loads just below the elastic limit, interlamellar cracks are formed within some colonies that are difficult to find because the amount of crack opening is very small. Hence, it is very hard to obtain valid crack growth data from observing the damage accumulation on the specimen surface.[17] Therefore, cracks emanating from micronotches were studied instead.

Flat hourglass specimens were used with a total length of 32.5 mm, a width of 4 mm in the gauge section and a thickness of 2.3 mm. The radius of curvature of the side notches was chosen in such a way that the area of observation (i.e. area of constant stress) was maximized (altogether 33 mm^2) and the stress concentration factor at midsection was minimized to $\alpha_k = 1.03$. Figure 6 shows the geometry and the stress field in the specimen.

Kinked ellipsoidal micronotches were placed at predefined locations in the observation area using fs laser ablation. Figure 7 shows an example of a prepared specimen with micronotches.

The specimens were subjected to load-controlled cyclic loading in fully reversed loading condition with maximum load just below the elastic limit. Periodic scans of the observation area were made during the test using a travelling long-distance optical microscope. Thus, the damage accumulation process on the surface could be

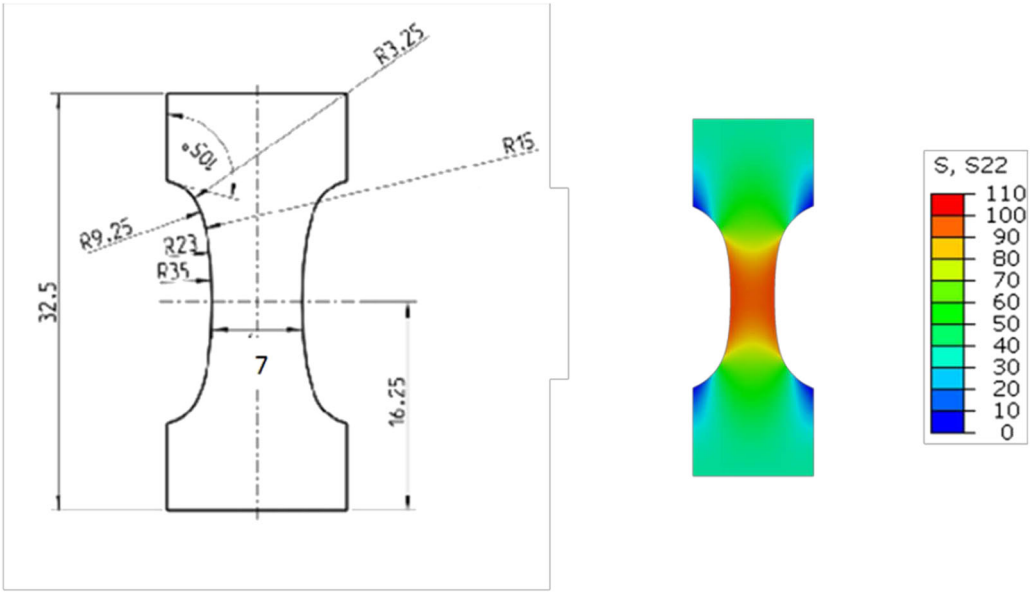

Fig. 6 Specimen geometry and finite element analysis of specimen, normal stresses at 100 MPa.

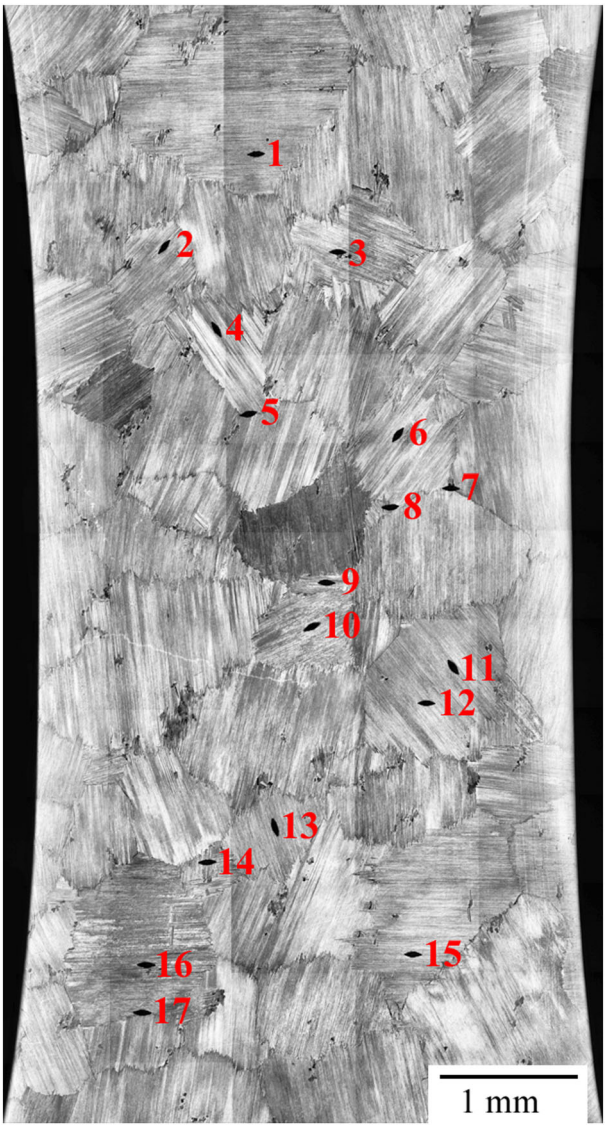

Fig. 7 γ-TiAl specimen containing micronotches.

closely monitored. In particular, it was possible to simultaneously observe crack initiation and crack growth for all the active micronotches on the surface of a given specimen.

MICROCRACK INITIATION AND GROWTH

Altogether, three specimens containing 30 micronotches were tested. Similar to the examples shown in Fig. 7, the manufactured micronotches were placed within a colony (see, e.g. notch #10 in Fig. 7) or on a colony boundary (example notch #7 in Fig. 7) with some notches being oriented in a direction parallel to the lamellae (e.g. notch #11 in Fig. 7) and others perpendicular to the loading direction irrespective of the lamellae orientation (e.g. notch #12 in Fig. 7). Observable microcracks were initiated from about 39% of the notches. All of the cracks propagated parallel to the lamella direction, if the notches in question were placed within a lamella colony, or sometimes also along the colony boundary, if the root of the crack-initiating notch was placed there. Figure 8 shows the microcrack initiated from notch #15 as a typical example.

The crack velocity within one colony was rather high, typically up to 10^{-2} mm cycle^{-1} or even higher, but could still be resolved with the given equipment by taking frequent scans. The observed crack paths (Figs 8 & 9) and the large amount of scatter (Fig. 10) in the crack growth rate indicate that the cracks emanating from micronotches were indeed microstructurally small cracks similar to those that are initiated in the material without a starter notch. This is confirmed by the fact that there is no significant difference between the crack growth rates of notch-initiated cracks (full symbols in Fig. 10) and those of natural cracks (open symbols in Fig. 10). Note that the title on the y-axis in Fig. 10 reads 'da/dN' in agreement with a standard notation, but actually, the projected value of the surface-crack length c is depicted. The range of the stress intensity factor K was determined for each crack using the stress intensity factor for semi-elliptical cracks with the crack length c on the surface defined as the projected length perpendicular to the loading axis and the depth a determined from the equilibrium value of the aspect ratio $a/c = 0.825$. All tests were performed under fully reversed loading ($R = -1$); hence, $K = K_{max}$.

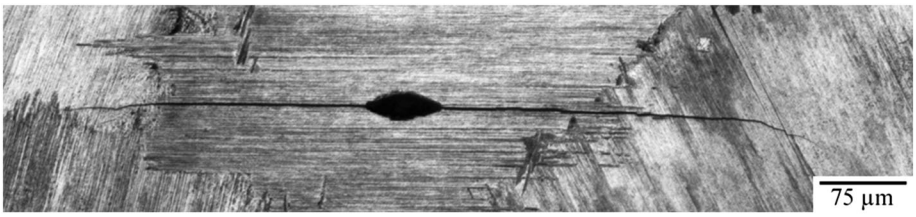

Fig. 8 Crack initiated from micronotch #15.

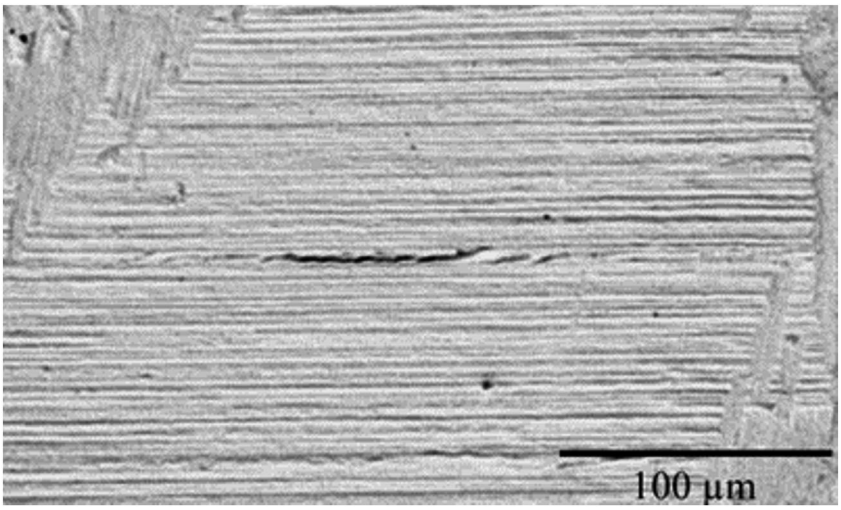

Fig. 9 Microcrack initiated without a starter notch.

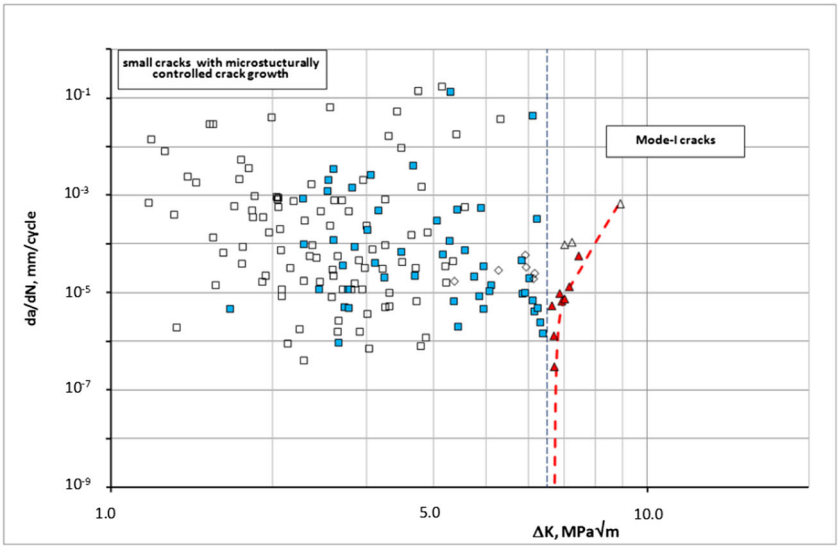

Fig. 10 Crack growth rates in fully lamellar γ-TiAl; full symbols, cracks initiated from micronotches; hollow symbols, no additional starter notch; □, microcracks with visible interaction with the lamellae; ◊, intermediate cracks with partial translamellar mode-I extension; Δ, mode-I cracks (long cracks grown from microcracks); - - -, estimated crack growth law for long cracks.

Most microcracks were stopped at the first colony boundary. If this first barrier was breached, the crack growth velocity increased rapidly and failure was imminent. After crossing the colony boundary, cracks generally extended in a translamellar mode perpendicular to the applied load; that is, they became long fracture mechanics cracks.

CONCLUSION

Micronotches can be introduced into a material using fs laser ablation. These notches act as crack-starting elements and can be used to initiate well-defined small cracks, which interact with the surrounding microstructure. Kinked ellipsoidal notches with a trailing kink in the notch contour trigger crack initiation in a very controlled way. It has been shown that cracks generated by this method are microstructurally short cracks, which interact with the microstructural barriers in the material; that is, intermittent crack growth can be studied in a controlled way.

Micronotches machined by fs laser ablation are competing with controlled microcrack initiation using FIB. The advantage of laser machining lies in considerably shorter machining times (fs laser takes less than 7 min for the notches used here, whereas an FIB notch of

comparable size takes at least 40 min or even longer) and controlled ablation in depth direction due to adjustable ablation energy. The last point is very important when kinked notch contours are made. A further advantage is that ablated material can be easily removed using some blowing device with air. The FIB machining, on the other hand, has the advantage that the micronotch can be positioned very precisely in the microstructure using a high-solution scanning electron microscope, whereas an optical microscope is part of the laser-machining device. At present, contours containing features with dimensions below 1–2 μm are beyond the resolution power of the laser system used, whereas very fine features can be easily introduced with the FIB.

Acknowledgements

Financial support of the German National Science Foundation (DFG) is gratefully acknowledged. Valuable contributions were made by E. Merdian and C. Scarpe within the framework of their theses. The material was provided by Chinese Iron and Steel Institute in Beijing, China (Dr Xin-yue Huang).

REFERENCES

1 Wessel, W., Brueckner-Foit, A., Mildner, J., Englert, L., Haag, L., Horn, A., Wollenhaupt, M. and Baumert, T. (2010) Use of femtosecond laser-induced breakdown spectroscopy (fs-LIBS) for micro-crack analysis on the surface. *Engng Fract. Mech*., **77**, 1874–1883.

2 Brueckner-Foit, A., Besel, M. and Zeismann, F. (2009) Fatigue properties of a graded steel component. In: *Proceedings of ASME International Mechanical Engineering Congress & Exposition IMECE*, Lake Buena Vista, Florida, USA, November 13-19.

3 Oguma, H. and Nakamura, T. (2011) Influence of environment on the formation of unique morphology on fracture surface in sub-surface fractures. *Paper pres. at VHCF 5*, Berlin, Germany.

4 Kruzic, J. J., Campbell, J. P. and Ritchie, R. O. (1999) On the fatigue behavior of γ- based titanium aluminides: role of small cracks. *Acta Mater*., **47**, 801–816.

5 Inkson, B. J., Mulvihill, M. and Möbus, G. (2001) 3D determination of grain shape in a FeAl-based nanocomposite by 3D FIB tomography. *Scr. Mater*., **2001**, 45, 753–758.

6 Wu, H. Z., Robert, S. G., Mobus, G. and Inkson, B. J. (2003) Subsurface damage analysis by TEM and 3D FIB crack mapping in alumina and alumina/5vol.%SiC nanocomposites. *Acta Mater*., **51**, 149–163.

7 Shyam, A., Jones, J. W. and Allison, J. E. (2006) On small fatigue crack growth in structural materials. In: *Proceedings of the 9th International Fatigue Congress*, Atlanta, Georgia, USA.

8 Shyam, A., Allison, J. E. and Jones, J. W. (2005) A small fatigue crack growth relationship and its application to cast aluminum. *Acta Mater*., **53**, 1499–1509.

9 Shyam, A., Picard, Y. N., Jones, J. W., Allison, J. E. and Yalisove, S. N. (2004) Small fatigue crack propagation from micronotches in the cast aluminum alloy W319. *Scr. Mater*., **50**, 1109–1114.

10 Motoyashiki, Y., Brueckner-Foit, A., Englert, L., Haag, L., Wollenhaupt, M. and Baumert, T. (2006) Use of femtosecond laser technique for studying physically small cracks. *Int. J Fract*., **139**, 561–568.

11 Pippan, R., Zegler, C., Gach, W., Bichler, C. and Weinhandl, H. (2011). On the mechanism of fatigue crack propagation in ductile metallic materials. *Int. J. Fatigue Fract. Eng Mater. Struct*., **34**, 1–16.

12 Pokluda, J., Pippan, R., Vojtek, T. and Hohenwarter, A. (2014). Near-threshold behaviour of shear-mode fatigue cracks in metallic materials. *Int. J. Fatigue Fract. Eng Mater. Struct*., **37**, 232–254.

13 Weikert, M. (2005) *Oberflächenstrukturieren mit ultrakurzen Laserpulsen* (in German). Herbert Utz Verlag, München, Germany.

14 Nolte, S., Kamlage, G., Korte, F., Bauer, T., Wagner, T., Ostendorf, A., Fallnich, C. and Welling, H. (2000) Microstructuring with femtosecond lasers. *Adv. Eng. Mater*., **2**, 23–27.

15 Korte, F., Adams, S., Egbert, A., Fallnich, C., Ostendorf, A., Nolte, S., Will, M., Ruske, J. P., Chichkov, B. N. and Tünnermann, A. (2000) Sub-diffraction limited structuring of solid targets with femtosecond laser pulses. *Opt. Express*, **7**, 41–49.

16 Shannon, J. L. and Munz, D. (1984) Specimen size and geometry effects on fracture toughness of aluminum oxide measured with short-rod and short-bar chevron-notched specimens. Chevron-Notched Specimens: Testing and Stress Analysis. *ASTM STP 855*, 270–280.

17 Wessel, W. (2011) Mikrostrukturelle Untersuchungen der Rissinitiierung und -ausbreitung in intermetallischen TiAl-Legierungen unter zyklischer und quasistatischer Belastung (in German), *Ph.D. Thesis*, University of Kassel, Germany.